

# Dispersion interactions and reactive collisions of ultracold polar molecules

Svetlana Kotochigova\*

*Department of Physics, Temple University, Philadelphia, PA 19122-6082, USA*

Progress in ultracold experiments with polar molecules requires a clear understanding of their interactions and reactivity at ultra-low collisional energies. Two important theoretical steps in this process are the characterization of interaction potentials between molecules and the modeling of reactive scattering mechanism. Here, we report on the *ab initio* calculation of isotropic and anisotropic van der Waals interaction potentials for polar KRb and RbCs colliding with each other or with ultracold atoms. Based on these potentials and two short-range scattering parameters we then develop a single-channel scattering model with flexible boundary conditions. Our calculations show that at low temperatures (and in absence of an external electric field) the reaction rates between molecules or molecules with atoms have a resonant character as a function of the short-range parameters. We also find that both the isotropic and anisotropic van der Waals coefficients have significant contributions from dipole coupling to excited electronic states. Their values can differ dramatically from those solely obtained from the permanent dipole moment. A comparison with recently obtained reaction rates of fermionic  $^{40}\text{K}^{87}\text{Rb}$  shows that the experimental data can not be explained by a model where the short-range scattering parameters are independent of the relative orbital angular momentum or partial wave.

## I. INTRODUCTION

Recent advances in creating ultracold polar molecules in the lowest rovibrational ground state [1, 2] have created a new scientific playground for studying quantum phenomena that govern collisions and interactions between molecules at low temperatures. Some key theoretical insights into the dipolar character of these interactions have already been developed over the last few years [3–9]. It was shown that dipole-dipole forces can be quite strong and may give rise to complex many-body physics in cold polar gases. Molecules with dipole moments, which interact via very long-range dipolar forces when oriented in an external electric field, can form strongly correlated condensed matter-like systems, realize effective spin models, and create field-linked states [9–12].

Currently, there is also significant interest in investigations of scattering properties of ultracold molecules. It is expected that such properties will be very different when molecules are held in optical dipole traps or when held in individual sites of an optical lattice. Holding molecules in individual sites of an optical lattice prevents them from approaching each other and allow dipole-dipole forces to play a dominant role in interactions between polar molecules [13, 14]. Intriguingly, in lower dimensional systems, where tight confinement along one or

---

\* E-mail:skotoch@temple.edu

more spatial directions is applied, dipole forces can be engineered to be non-destructive or repulsive and collective effects are predicted [15–18]. For example, Ref. [17] has suggested a technique that decreases inelastic collisional rates and enhances elastic collisional rates using a combination of external electric and microwave fields in a two-dimensional lattice.

In a three-dimensional trapping environment molecules can scatter freely. Generally, polar molecules are expected to be very fragile to the destructive nature of these collisions. There is experimental evidence of the significant role that such collisions play in defining molecular lifetimes [19–23]. The physical origin of this loss are rovibrational relaxations and reactive collisions, both of which occur at short-range, when the molecules are close together. An understanding and quantitative description of these collisions might help define conditions under which an ultracold molecular system is long lived. Furthermore, learning about the short-range region will help to unravel the role of reactivity in ultracold collisions.

The effect of reactivity on the molecular lifetime at ultracold temperatures, with a few exceptions [23, 24], remains largely unexplored. References [25–28] are devoted to theoretical developments towards a full quantum dynamics calculation of reactive collisions with cold molecules. The quantum mechanical description of reactions is challenging due to the complex nature of the differential equations and boundary conditions as well as difficulties with generating potential surfaces of sufficient quality for three and four-atomic systems. The most successful theories are associated with light atom-diatom systems [29–31] that are of astrophysical interest, can be Stark decelerated, or cooled with a buffer gas. Recently, extensive quantum scattering calculations in Refs. [25, 32, 33] have shown significant influence of so-called ‘virtual states’ in the entrance channel of the collision complex.

The interaction of molecules without an external electric field is dominated by the dispersive van der Waals forces rather than dipole-dipole interactions. At low temperatures quantum mechanical effects play a prominent role in the molecular scattering from such potentials and are crucial for the description of the interplay between inelastic and elastic collisional rates. The present study explores these dispersion interactions, which act at short- to medium-range, and introduces a scattering model of ultracold polar alkali-metal molecules. We use a characteristic length scale to distinguish between the dispersion and short-range interaction regions. The short-range boundary, which defines the lower limit of the scattering model, is described by  $C_6^{\text{iso}}/R_{\text{sr}}^6 \ll 2B_e$ , where  $C_6^{\text{iso}}/R_{\text{sr}}^6$  is the isotropic dispersion potential and  $B_e$  is the rotational constant of the ground state molecule. The short-range separation  $R_{\text{sr}}$  must be smaller than the isotropic van der Waals length  $R_6 = (2\mu C_6^{\text{iso}}/\hbar^2)^{1/4}$ , where  $\mu$  is the reduced mass of the molecules. An accurate estimate of these characteristic length scales for KRb and RbCs will be given below.

Our scattering model is an extension of the theory developed by Mies and Julienne [34, 35]. Here we modified this scattering theory by making the short-range boundary conditions more flexible by assuming that not all molecules that penetrate to short-range will be lost. This allows us to introduce two short-range parameters linked to the rovibrational structure of exit reaction channels. Recently, a model based on quantum defect theory has been introduced in Ref. [24], which accounts for the short-range interactions by connecting a complex valued or optical potential to the van der Waals potential.

Since our scattering theory is solely based on the dispersion interaction potentials, we first calculate molecule-molecule and atom-molecule van der Waals coefficients by integrating products of the dynamic polarizability over imaginary frequencies. Unlike for atom-atom interactions molecular interactions depend on their rotational and vibrational state and can

have contributions from transitions within the ground state potential as well as from the electronically excited spectrum. For polar molecules the former contribution is nonzero, even for levels with a well defined angular momentum while the excited-state contribution can be significant. The excited contribution is often missing in the analyses of short-range molecular interactions [17, 36].

The paper is organized as follows. In section II we describe the theory of dispersion interaction isotropic and anisotropic potentials between molecules and molecules with atoms. The numerical potentials and van der Waals coefficients are obtained for the X  $^1\Sigma^+$  ground state of KRb and RbCs as a function of its vibrational quantum number and presented in Section III. Section IV gives basics of our scattering model and provide examples of the inelastic scattering rates for ultracold colliding molecules. The last Section V summarizes essential conclusions of the presented research.

## II. DISPERSION POTENTIALS FOR THE MOLECULAR INTERACTION

We describe the dispersion interaction potential between molecules  $A$  and  $B$ , each in a rovibrational level  $|X, vJM\rangle \equiv |i, M\rangle$  of their X electronic ground state, by assuming that the molecules are far apart and their wavefunctions do not overlap. Here, the magnetic quantum number  $M$  is the projection along a laboratory fixed coordinate system of their total angular momentum  $\vec{J}$  and  $i$  describes all other quantum labels. Their energy  $E_i$  only depends on the label  $i$  and not on  $M$ . These assumptions allow us to use a (degenerate) second-order perturbation theory similar to that described by Ref. [37]. For two molecules the matrix elements of the dispersion potential between the product states  $|i_A, M_A; i_B, M_B\rangle \equiv |i_A, M_A\rangle|i_B, M_B\rangle$  and  $|i_A, M'_A; i_B, M'_B\rangle$  with different projection quantum numbers but the same angular momenta  $J_A$  and  $J_B$  are

$$U_{\text{disp}}(\vec{R}) = - \sum_{\substack{S_A \neq i_A, M_A \\ S_B \neq i_B, M_B}} \frac{\langle i_A, M_A; i_B, M_B | V_{dd} | S_A; S_B \rangle \langle S_A; S_B | V_{dd} | i_A, M'_A; i_B, M'_B \rangle}{E_{S_A} + E_{S_B} - (E_{i_A} + E_{i_B})}, \quad (1)$$

where the sums  $S_A$  and  $S_B$  are over all electronic, rovibrational, continuum states of molecules  $A$  and  $B$ , respectively, restricted to states with energy  $E_{S_A} + E_{S_B} \neq E_{i_A} + E_{i_B}$ . The operator  $V_{dd}$  is the dipole-dipole interaction Hamiltonian [37]

$$V_{dd}(\vec{R}) = -\sqrt{30} \sum_{m_1 m_2 m} \begin{pmatrix} 1 & 1 & 2 \\ m_1 & m_2 & m \end{pmatrix} d_{1m_1}^A d_{1m_2}^B \frac{C_{2m}(\hat{R})}{R^3}, \quad (2)$$

where  $d^A$  and  $d^B$  are the two rank-1 spherical dipole operators of the molecules and  $\vec{R}$  is the separation between and orientation of the two molecules with respect to a laboratory axis. The  $\begin{pmatrix} \dots \end{pmatrix}$  is a Clebsch-Gordan coefficient and  $C_{lm}(\hat{R})$  is the modified spherical harmonic function [38]. Inserting Eq. (2) into Eq. (1) and after a number of transformations following Ref. [37] we find that the dispersion potential is the sum of the isotropic  $U_{\text{disp,iso}}(\vec{R})$  and anisotropic  $U_{\text{disp,aniso}}(\vec{R})$  potentials, which can be expressed in terms of the molecular dynamic polarizability tensor at imaginary frequency,  $\alpha^{A/B}(i\omega)$ , of molecule  $A$  and  $B$ .

We find an isotropic  $U_{\text{disp,iso}}(\vec{R})$  potential

$$U_{\text{disp,iso}}(R) = -\frac{C_6^{\text{iso}}}{R^6} \delta_{M_A, M'_A} \delta_{M_B, M'_B} - \frac{C_{6,22}^{\text{iso}}}{R^6} \langle i_A, M_A; i_B, M_B | T_{0,0}(2, 2) | i_A, M'_A; i_B, M'_B \rangle, \quad (3)$$

where the rank- $l$  tensor operator  $T_{l,m_l}(k, p)$  is defined by

$$\begin{aligned} \langle i_A, M_A; i_B, M_B | T_{l,m_l}(k, p) | i_A, M'_A; i_B, M'_B \rangle &= \frac{1}{N_l(k, p)} \sum_{qr} \langle lm_l | k p q r \rangle \\ &\times \langle J_A M_A | J_A k M'_A q \rangle \langle J_B M_B | J_B p M'_B r \rangle \end{aligned} \quad (4)$$

and the normalization  $N_l(k, p) = \langle l0 | k p 00 \rangle \langle J_A J_A | J_A k J_A 0 \rangle \langle J_B J_B | J_B p J_B 0 \rangle$ , such that the operator  $\langle \dots | T_{l,m_l}(k, p) | \dots \rangle$  is one for the stretched state  $|i_A, M_A\rangle = |i_A, M'_A\rangle = |X, v J_A J_A\rangle$  and  $|i_B, M_B\rangle = |i_B, M'_B\rangle = |X, v J_B J_B\rangle$ . Here  $\langle j_3 m_3 | j_2 j_1 m_2 m_1 \rangle$  is a Clebsch-Gordan coefficient. Consequently,

$$\begin{aligned} C_6^{\text{iso}} &= \frac{3}{\pi} \int_0^\infty d\omega \langle i_A, J_A | \bar{\alpha}^A(i\omega) | i_A, J_A \rangle \langle i_B, J_B | \bar{\alpha}^B(i\omega) | i_B, J_B \rangle \\ C_{6,22}^{\text{iso}} &= \frac{3}{45\pi} \int_0^\infty d\omega \langle i_A, J_A | \Delta\alpha^A(i\omega) | i_A, J_A \rangle \langle i_B, J_B | \Delta\alpha^B(i\omega) | i_B, J_B \rangle \end{aligned}$$

where, for each molecule  $A$  and  $B$ ,  $\bar{\alpha} = (\alpha_{xx} + \alpha_{yy} + \alpha_{zz})/3$  and  $\Delta\alpha = \alpha_{zz} - (\alpha_{xx} + \alpha_{yy})/2$  are given in terms of diagonal  $x$ ,  $y$ , and  $z$  components of the polarizability tensor at imaginary frequency. For atoms and diatoms the polarizability tensor is fully determined by  $\bar{\alpha}$  and  $\Delta\alpha$ .

The anisotropic van der Waals potential is defined by

$$\begin{aligned} U_{\text{disp,aniso}}(\vec{R}) &= \frac{1}{R^6} \sum_{m_l} (-1)^{m_l} C_{2m_l}(\hat{R}) \left\{ C_{6,02}^{\text{aniso}} \langle i_A, M_A; i_B, M_B | T_{2,-m_l}(0, 2) | i_A, M'_A; i_B, M'_B \rangle \right. \\ &\quad + C_{6,20}^{\text{aniso}} \langle i_A, M_A; i_B, M_B | T_{2,-m_l}(2, 0) | i_A, M'_A; i_B, M'_B \rangle \\ &\quad \left. + C_{6,22}^{\text{aniso}} \langle i_A, M_A; i_B, M_B | T_{2,-m_l}(2, 2) | i_A, M'_A; i_B, M'_B \rangle \right\} \end{aligned}$$

and the van der Waals coefficients are

$$\begin{aligned} C_{6,02}^{\text{aniso}} &= -\frac{1}{\pi} \int_0^\infty d\omega \langle i_A, J_A | \bar{\alpha}^A(i\omega) | i_A, J_A \rangle \langle i_B, J_B | \Delta\alpha^B(i\omega) | i_B, J_B \rangle, \\ C_{6,20}^{\text{aniso}} &= -\frac{1}{\pi} \int_0^\infty d\omega \langle i_A, J_A | \Delta\alpha^A(i\omega) | i_A, J_A \rangle \langle i_B, J_B | \bar{\alpha}^B(i\omega) | i_B, J_B \rangle, \\ C_{6,22}^{\text{aniso}} &= \frac{2}{7} C_{6,22}^{\text{iso}}. \end{aligned}$$

In our framework the  $x$ ,  $y$ , and  $z$  component of the diagonal dynamic polarizability at imaginary frequency is determined as

$$\langle i, M | \alpha_{nn}(i\omega) | i, M \rangle = \frac{1}{\epsilon_0 c} \sum_{S \neq i, M} \frac{(E_S - E_i)}{(E_S - E_i)^2 - (i\hbar\omega)^2} \times |\langle S | \vec{d} \cdot \hat{n} | i, M \rangle|^2 \quad (5)$$

where  $\hat{n}$  is the unit vector along the  $n=x, y$ , and  $z$  direction, and  $i, M$  and  $S$  denote rovibrational wave functions of a single molecule,  $\langle S | \vec{d} | i, M \rangle$  are matrix elements of permanent or transition electronic dipole moments. Equation (5) includes a sum over the dipole transitions to the rovibrational levels within the ground-state potential as well as to the rovibrational levels of electronically-excited potentials. Contributions from scattering or continuum states

of the electronic potentials are also included. Finally,  $c$  is the speed of light and  $\epsilon_0$  is the electric constant.

In summary, we have found various contributions to the long-range van der Waals potential. They are characterized by their angular momentum dependence. In particular, the term proportional to  $C_6^{\text{iso}}$  is independent of magnetic projections and the relative orbital angular momentum between the molecules. The term proportional to  $C_{6,22}^{\text{iso}}$  induces coupling between the magnetic projections of the two molecules without affecting the relative orbital angular momentum. Finally, the three  $C_6^{\text{aniso}}$  contributions do cause mixing between magnetic projections and relative orbital angular momentum. Note that the coefficients  $C_{6,22}^{\text{iso}}$  and  $C_{6,22}^{\text{aniso}}$  will be of the same order of magnitude. They both are proportional to a product of two  $\Delta\alpha$ . Dispersion terms proportional to the spherical harmonic  $C_{lm}(\hat{R})$  for  $l > 2$  also exist. We do not consider them here as they are smaller.

### III. VAN DER WAALS COEFFICIENTS OF POLAR MOLECULES

This section describes our results for the van der Waals coefficients  $C_6^{\text{iso}}$  and  $C_6^{\text{aniso}}$  between two polar KRb dimers and two RbCs dimers. These molecules are prepared in rovibrational states of the ground  $X^1\Sigma^+$  potential and are of interest for on-going ultracold experiments [1, 2, 23, 41]. We have used a non-relativistic *ab initio* version of the electronic structure multi-reference configuration interaction method [39, 40] to obtain potential energies, permanent and transition electric dipole moments of the KRb and RbCs molecules as a function of internuclear separation. In order to determine experimental observables we combine our electronic structure calculations with that of the calculation of rotational-vibrational energy levels to find vibrationally-averaged transition dipole moments.

The isotropic  $C_6^{\text{iso}}$  coefficients between two molecules both in the  $J=0$  rotational levels of the  $X^1\Sigma^+$  ground state potential as a function of vibrational quantum number are shown in Fig. 1. Comparison of the two panels show that for the deeply bound  $J=0$  vibrational levels the isotropic coefficient for RbCs is almost an order of magnitude larger than for KRb. This is because for these levels the main contribution to the total value of  $C_6^{\text{iso}}$  is due to transitions within the ground state potential, which to good approximation is equal to  $d_v^4/(6B_v)$  [36], where  $d_v$  and  $B_v$  are the vibrationally averaged permanent dipole moment and rotational constant of level  $v$ , respectively. The permanent dipole moment of RbCs is twice as large as that of KRb, while  $B_v$  is almost half the size [2, 39, 42]. The permanent dipole moment of both molecules rapidly decreases to zero with  $v$  and the  $X^1\Sigma^+$  contribution to the van der Waals coefficient follows this trend. Consequently, for the highly excited vibrational levels the  $C_6^{\text{iso}}$  are solely determined by transitions to electronically excited states. In fact, for KRb the excited state contribution plays a dominant role for all  $v$ .

Figure 1 also shows the  $J=1$  isotropic dispersion coefficients. These are independent of the projection quantum number  $M$ . In this case the contributions from the transitions from  $J=1$  to  $J=0$  and 2 within the ground state potential have opposite sign and nearly cancel each other. As a result, the value of  $C_6^{\text{iso}}$  is close or equal to the value obtained by only including the excited state contributions. The dispersion coefficient is weakly dependent on  $v$ . The isotropic values for the  $v = 0$  vibrational level of the  $X^1\Sigma^+$  state of KRb and RbCs are given in Table I.

The  $J=0$  and 1 dispersion coefficients are the same when they are solely determined by transitions to electronically excited states. This is because rotational energy splittings are

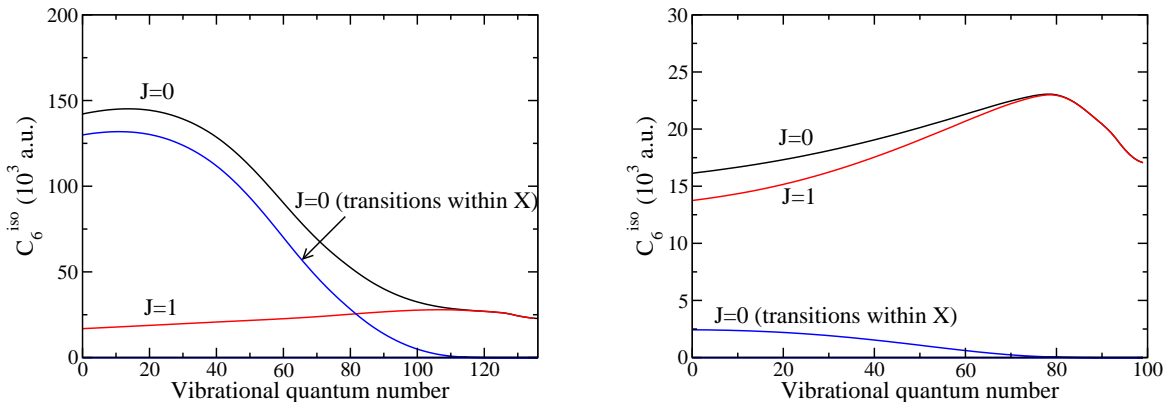


FIG. 1: Isotropic molecule-molecule van der Waals coefficients in atomic units for the  $J=0$  and 1 rotational levels of the  $X^1\Sigma^+$  ground state of RbCs (left panel) and KRb (right panel) as a function of vibrational quantum number. The curves labeled “ $J = 0$  (transitions within X)” correspond to an isotropic van der Waals coefficient where only contributions from transitions to ro-vibrational levels of the  $X^1\Sigma^+$  potential are included.

negligible compared to electronic excitation energies and the rotational energy dependence of  $E_{S_A}$  and  $E_{S_B}$  in Eq. 1 can be neglected. Alternatively, this independence follows from a simple atomistic model for the dispersion coefficient of weakly bound molecules. The molecular electronic wave functions are then to good approximation products of atomic electronic wave functions and the molecule-molecule dispersion coefficient reduces to a sum of atom-atom dispersion coefficients, which do not depend on the rotational state of the molecule. In fact, for RbCs+RbCs we find that  $C_6^{\text{iso}} \rightarrow 2C_6(\text{RbCs}) + C_6(\text{Rb}_2) + C_6(\text{Cs}_2) = 22868$  a.u. for large  $v$  using the well-characterized Rb+Rb, Rb+Cs, and Cs+Cs dispersion coefficients [43]. This value is in good agreement with our results. A similar agreement is found for  $C_6^{\text{iso}}$  of the interacting KRb molecules based on values of  $C_6$  from [43].

The collisions between two  $J=1$  molecules are anisotropic. Once molecules are prepared in the specific state characterized by  $M$ , the interaction energy can depend on the relative orientation of the two molecules. In fact, the anisotropic interaction can change the projection quantum numbers. Figure 2 (left panel) shows our results for the anisotropic  $C_{6,02}^{\text{aniso}}$  coefficient as a function of vibrational quantum number for  $J = 1$  rotational sublevels,  $M = 0$  and  $M = \pm 1$ , of the  $X^1\Sigma^+$  ground state of KRb and RbCs. The anisotropy for RbCs changes sign as function of  $v$  due to competing contributions from the ground and excited states. In both cases  $C_{6,02}^{\text{aniso}}$  goes to zero for highly excited vibrational levels. For these collision we have  $C_{6,20}^{\text{aniso}} = C_{6,02}^{\text{aniso}}$ .

Our predicted isotropic van der Waals  $C_6^{\text{iso}}$  coefficients for the interaction between KRb molecules have been used in theoretical models [23, 24] to successfully describe the loss rate constant  $\mathcal{K}$  observed in a JILA experiment as a function of temperature [23]. The anisotropic  $C_6^{\text{aniso}}$  coefficients can be used for describing collisions between molecules in non-zero  $J$  rotational states. Our estimate shows that an experimentally-accessible external electric field of 2 kV/cm will induce an  $\approx 50$  MHz splitting between  $M = 0$  and  $M = \pm 1$  components of  $J = 1$  rotational state of KRb. The anisotropic interaction terms, for example, with coefficient  $C_{6,02}^{\text{aniso}} \approx 2500$  a.u., will then cause a reorientation of the magnetic sublevels for separations less than  $80 a_0$  and will contribute to loss of molecules from the

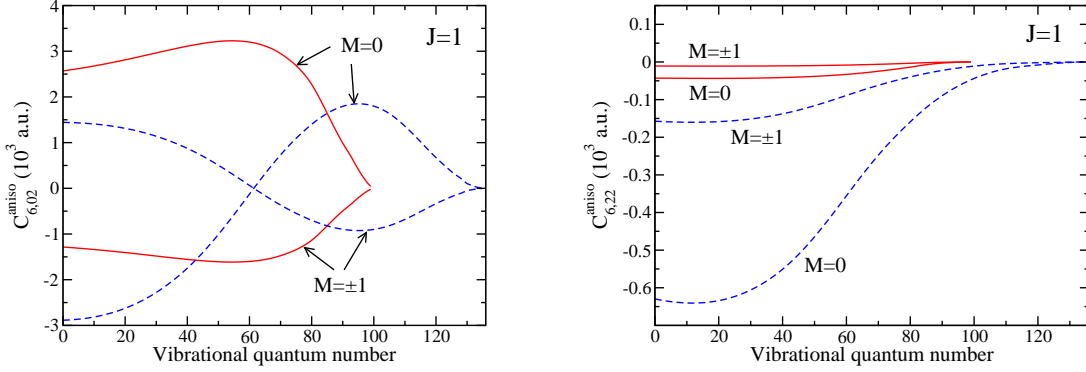


FIG. 2: Anisotropic van der Waals coefficients  $C_{6,02}^{\text{aniso}}$  (left panel) and  $C_{6,22}^{\text{aniso}}$  (right panel) in atomic units as a function of vibrational quantum number for two molecules in a  $J = 1$  rotational levels of the  $X^1\Sigma^+$  ground state of KRB (solid lines) and RbCs (dashed lines). The coefficient is shown for both  $M = 0$  and  $1$ . The coefficient for  $M = 0$  follows from the one for the stretched state  $M = 1$  by evaluation of the tensor  $T_{lm_i}$  in Eq. 4.

trap.

We also determined the coefficients  $C_{6,22}^{\text{iso}}$  and  $C_{6,22}^{\text{aniso}}$ . For rotationless  $J = 0$  molecules both coefficient are zero. Right panel of Fig. 2 shows  $C_{6,22}^{\text{aniso}}$  for  $J = 1$  as function of vibrational quantum number. These values are an order of magnitude smaller than the contributions discussed so far. The anisotropic coefficients for both molecules in the  $v = 0$   $X^1\Sigma^+$  state are given in Table I.

It was observed in Refs. [19–23] that the lifetime of both Feshbach and deeply bound polar molecules decreases when they are in the presence of ultracold atoms. This suggests that collisions between atoms and molecules play a role in limiting the molecule lifetime. These losses are due to relaxation of rovibrational or hyperfine degrees of freedom that have enough kinetic energy to remove both molecule and atom from an external optical or magnetic trap. Another possible loss channel is an ultracold chemical reaction. To understand these losses, we determine the isotropic and anisotropic van der Waals coefficients for the interaction between a molecule in state  $|i_{\text{Mol}}, M_A\rangle$  and atom in state  $|i_{\text{At}}, M_B\rangle$ . Again following Ref. [37], the isotropic coefficient is

$$C_6^{\text{AtMol,iso}} = \frac{3}{\pi} \int_0^\infty d\omega \langle i_{\text{Mol}}, J_A | \bar{\alpha}^{\text{Mol}}(i\omega) | i_{\text{Mol}}, J_A \rangle \langle i_{\text{At}}, J_B | \bar{\alpha}^{\text{At}}(i\omega) | i_{\text{At}}, J_B \rangle, \quad (6)$$

where  $\bar{\alpha}^{\text{Mol}}$  and  $\bar{\alpha}^{\text{At}}$  are the mean molecular and atomic polarizabilities, respectively. The anisotropic coefficient is

$$C_{6,20}^{\text{AtMol,aniso}} = \frac{1}{\pi} \int_0^\infty d\omega \langle i_{\text{Mol}} | \Delta\alpha^{\text{Mol}}(i\omega) | i_{\text{Mol}} \rangle \langle i_{\text{At}} | \bar{\alpha}^{\text{At}}(i\omega) | i_{\text{At}} \rangle, \quad (7)$$

The values for  $C_{6,22}^{\text{AtMol,iso}}$ ,  $C_{6,02}^{\text{AtMol,aniso}}$ , and  $C_{6,22}^{\text{AtMol,aniso}}$  are zero as  $\Delta\alpha$  is zero for an atom.

Figure 3 shows the isotropic van der Waals coefficients for RbCs and KRB molecules with constituent atoms of Cs, Rb and Rb, K, respectively. It provides evidence that the van der Waals coefficients for both  $J=0$  and  $1$  are nearly the same. This is due to the fact that

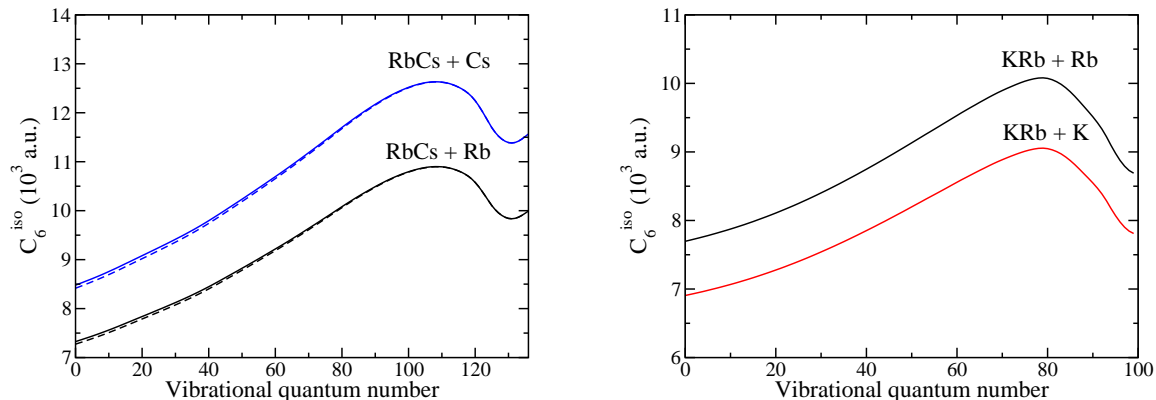


FIG. 3: Isotropic van der Waals coefficients in atomic units as a function of vibrational quantum number for the collision between a ground  $X^1\Sigma^+$  state RbCs molecule and either a Rb or Cs atom (left panel) and KRb molecule and either Rb or K atom (right panel). Rotational  $J=0$  (1) levels are shown as solid (dashed) lines, respectively. For KRb the  $J=0$  and 1  $C_6^{\text{iso}}$  coefficients are indistinguishable on the scale of a figure.

the contribution from transitions within the ground state are negligible. The lack of these contributions effects the behavior of an anisotropic  $C_6^{\text{AtMol,aniso}}$  coefficient as well. As it is shown in Fig. 4, the values of the  $C_6^{\text{AtMol,aniso}}$  for the same projections  $M$  have the same sign. Table I lists the isotropic and anisotropic values for the  $v = 0$  vibrational level of the  $X^1\Sigma^+$  state of KRb and RbCs with atoms.

Similar to the molecule-molecule dispersion potential, the van der Waals coefficients for one molecule and one atom are additive for a weakly-bound molecule. In other words, the  $C_6$  coefficient for the highly excited vibrational levels can be expressed as a sum of contributions from individual di-atoms. For example,  $C_6^{\text{RbCs+Rb,iso}} \rightarrow C_6(\text{RbCs}) + C_6(\text{Rb}_2) = 10035$  a.u. and  $C_6^{\text{RbCs+Cs,iso}} \rightarrow C_6(\text{RbCs}) + C_6(\text{Cs}_2) = 12514$  a.u [43] for weakly bound RbCs molecules. The agreement between the asymptotic values and our numerical calculations is satisfactory. The same estimate can be done for KRb molecules interacting at long distances with K or Rb atoms. This lead to  $C_6^{\text{KRb+Rb,iso}} \rightarrow C_6(\text{KRb}) + C_6(\text{Rb}_2) = 8965$  a.u. and  $C_6^{\text{KRb+K,iso}} \rightarrow C_6(\text{KRb}) + C_6(\text{K}_2) = 8171$  a.u., which agree within a few % with the numerical values of Fig. 3.

#### IV. REACTIVE COLLISIONS OF ULTRACOLD POLAR MOLECULES

The lifetime of ultracold molecules in an optical trap is determined by the inelastic collisional loss rates between these molecules. A collision can change the internal rovibrational state of the molecules as well induce reactions where the bonds between the atoms are rearranged. For example, for an ultracold KRb gas the reaction  $\text{KRb} + \text{KRb} \rightarrow \text{K}_2 + \text{Rb}_2$  is allowed [23]. Once the molecules are prepared in their absolute ground state only the reactive process is present.

This section describes our results using a quantum reflection model of the rate coefficient for rotationless  $J = 0$   $^{40}\text{K}^{87}\text{Rb}$  and  $^{85}\text{Rb}^{133}\text{Cs}$  ground state molecules. It is based on a modification of the approach developed in Refs. [34, 35]. We solve a single-channel radial Schrödinger equation for the inter-molecular separation with an isotropic van der Waals



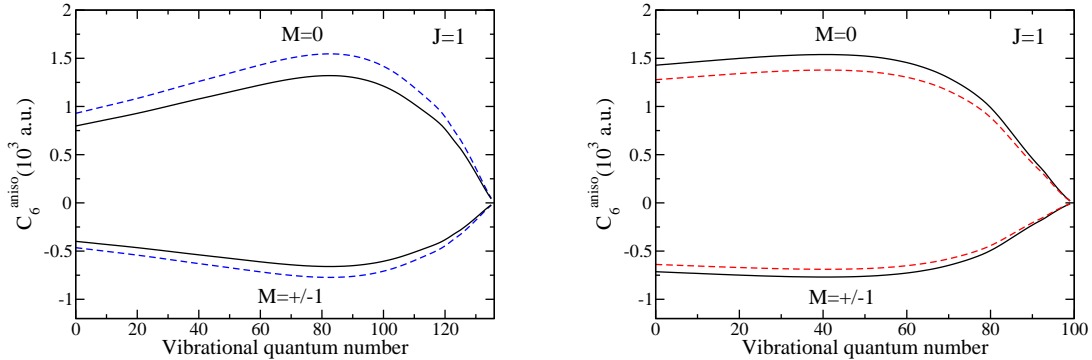


FIG. 4: Anisotropic van der Waals coefficients  $C_{6,20}^{\text{aniso}}$  in atomic units as a function of vibrational quantum number for  $J = 1$  rotational  $M = 0$  and  $M = \pm 1$  sublevels of the  $X^1\Sigma^+$  ground state of the RbCs+Rb (solid lines) and RbCs+Cs (dashed lines) interacting systems (left panel) and KRb+Rb (solid lines) and KRb+K (dashed lines) interacting systems (right panel).

potential for  $R > R_{\text{sr}}$ , where  $R_{\text{sr}}$  is a short-range separation to be defined below. Two short-range parameters describe the collisional wavefunction when the molecules are “close” together at  $R = R_{\text{sr}}$ . As we will show this boundary condition models the physics or reactivity for  $R < R_{\text{sr}}$  and “partially” inelastic events can occur. The short-range parameters can depend on the rovibrational state of the molecules. The isotropic van der Waals coefficients are taken from Table I. Recently, a similar model with a different treatment of the short-range interactions was used in Ref. [24] for the collisions between KRb molecules.

We use the van der Waals potential to determine the validity of the model and estimate characteristic length scales to distinguish between the dispersion and short-range interaction regions. The range of the isotropic van der Waals potential is defined as  $R < R_6 \equiv \sqrt[4]{2\mu C_6^{\text{iso}}/\hbar^2}$ , where  $\mu$  is the reduced molecular mass [44]. For  $v = 0$ ,  $J = 0$  KRb and RbCs molecules this separation is  $\approx 300 a_0$  and  $500 a_0$ , respectively. The short-range  $R_{\text{sr}}$  is defined by  $C_6^{\text{iso}}/R_{\text{sr}}^6 \approx 2B_v$ , where  $B_v$  is the rotational constant of the ground state molecule. For shorter separations the energy of the dispersion potential is much larger

TABLE I: Van der Waals coefficients in atomic units for the interaction between two molecules in the  $v = 0$ ,  $J = 0$  and 1 rovibrational levels of the  $X^1\Sigma^+$  potential as well as between such a molecule with an atom. The uncertainty in the coefficients is 5%.

System	$C_6^{\text{iso}}$		$C_{6,20}^{\text{aniso}}$		$C_{6,22}^{\text{aniso}}$	
	$J = 0$	$J = 1$	$(J, M) = (1, 0)$	$(J, M) = (1, \pm 1)$	$(J, M) = (1, 0)$	$(J, M) = (1, \pm 1)$
KRb + KRb	16133	13749	2569	-1285	-43	-11
RbCs + RbCs	142129	16865	1443	-2886	-630	-157
KRb + Rb	7696	7686	1428	-714		
KRb + K	6905	6896	1278	-639		
RbCs + Rb	7326	7274	798	-399		
RbCs + Cs	8479	8416	929	-465		

than the rotational energy and collisional interactions can mix rotational states. Such mixing falls outside the scope of our single channel description. We find values for  $R_{\text{sr}}$  between  $50 a_0$  and  $80 a_0$  for both molecules. Hence  $R_{\text{sr}} \ll R_6$ . In fact,  $C_6^{\text{iso}}/R_{\text{sr}}^6$  is much larger than collision energies of interest as well as the centrifugal potential  $\hbar^2 l(l+1)/(2\mu R_{\text{sr}}^2)$  between molecules. The quantum number  $l$  is the partial wave between the molecules or one molecule and one atom.

Our model involves scattering of rotationless molecules in the potential  $-C_6^{\text{iso}}/R^6 + \hbar^2 l(l+1)/(2\mu R^2)$  for  $R > R_{\text{sr}}$ . The contribution for partial wave  $l$  and projection  $m$  to the inelastic rate coefficient is given by

$$K_{lm}^{\text{loss}}(E) = v \frac{\pi}{k^2} \sum_{\alpha \neq i} |S_{i\alpha}(E, lm)|^2 = v \frac{\pi}{k^2} \left(1 - |S_{ii}(E, lm)|^2\right), \quad (8)$$

where  $E = \hbar^2 k^2/(2\mu)$  is the collision energy and  $v$  is the relative velocity. The scattering S matrix elements  $S_{i\alpha}(E, lm)$  describe the transmission and reflection amplitude from the initial state  $i$  of colliding molecules and atoms to a final state  $\alpha$  with either molecules in different rovibrational states or with a different bond. The sum over  $\alpha$  excludes the initial state. Flux conservation or the unitarity of the  $S$  matrix allows us to rewrite the loss rate coefficient in terms of the diagonal S matrix element,  $S_{ii}$ . At ultracold temperatures, only a few partial waves  $l$  contribute as for higher  $l$  the centrifugal barrier prevents the molecules from approaching each other and  $K_{lm}^{\text{loss}}$  rapidly goes to zero.

The scattering S matrix is calculated from the radial Schrödinger equation

$$\left(-\frac{\hbar^2}{2\mu} \frac{d^2}{dR^2} - \frac{C_6^{\text{iso}}}{R^6} + \frac{\hbar^2}{2\mu} \frac{l(l+1)}{R^2}\right) \psi_{lm}(R) = E \psi_{lm}(R)$$

at collision energy  $E$  with the boundary condition

$$\psi_{lm}(R) = A \left( e^{+i[y-\pi/4]} - \zeta_{lm}(E) e^{2i\delta_{lm}(E)} e^{-i[y-\pi/4]} \right) \quad (9)$$

at  $R = R_{\text{sr}} \ll R_6$ ,  $y = (R/R_6)^{-2}/2$ , and  $A$  is a normalization constant [44]. The exponents  $e^{\pm i[y-\pi/4]}$  can be recognized as WKB solutions of a van der Waals potential at zero collision energy. The short range amplitude  $\zeta_{lm}(E) e^{2i\delta_{lm}(E)}$  and thus the real parameters  $\zeta_{lm}(E)$  and  $\delta_{lm}(E)$  are not known a priori. They can only be determined from the chemical bonding between the three or four atoms. However, once they are known the boundary condition uniquely specifies the solution of the Schrödinger equation. Flux conservation requires that  $0 \leq \zeta_{lm} \leq 1$ , where  $\zeta_{lm} = 0$  corresponds to the case where no flux is returned from the short range and  $\zeta_{lm} = 1$  correspond to the case where everything is reflected back. The phase  $\delta_{lm}$  describes the relative phase shift of the flux that returns from  $R < R_{\text{sr}}$ . In Ref. [24] a model potential with an optical or imaginary term is used to describe the short range physics for  $R < R_{\text{sr}}$ .

The van der Waals potential is the largest energy scale at  $R = R_{\text{sr}}$  and, consequently, we *initially* assume that both  $\zeta_{lm}(E)$  and  $\delta_{lm}(E)$  are independent of collision energy  $E$ , partial wave  $l$ , and projection  $m$ . The validity of these approximations can only be tested by comparison with experimental data. We will do so with the data on KRb loss rate coefficients from Ref. [23].

In the limit  $R \rightarrow \infty$  the wavefunction approaches

$$\psi_l(R) \rightarrow e^{-i(kr-l\pi/2)} - S_{ii}(E, lm) e^{i(kr-l\pi/2)}, \quad (10)$$

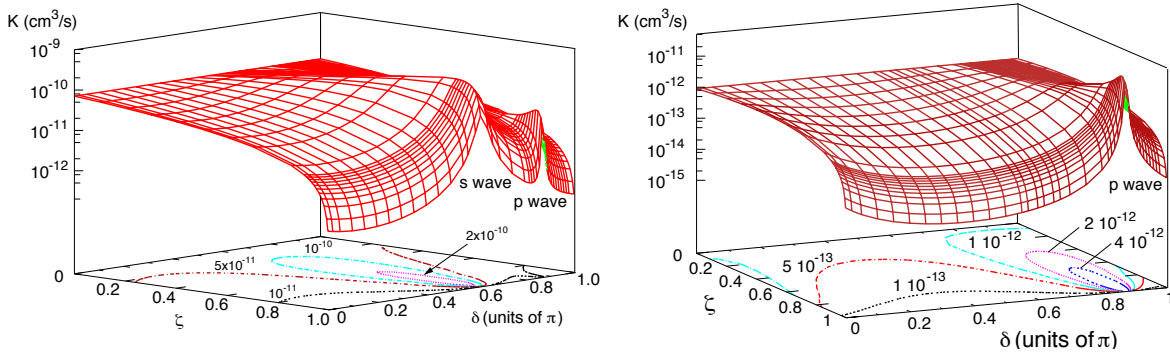


FIG. 5: The total inelastic loss rate coefficient for a nuclear spin unpolarized (left panel) and polarized (right panel) sample of  $v = 0$ ,  $J = 0$   $^{40}\text{K}^{87}\text{Rb}$  molecules in the  $X^1\Sigma^+$  potential as a function of the short-range parameters  $\zeta$  and  $\delta$  at a collision energy of  $E/k_B = 350$  nK. The loss rate of the unpolarized case contains non-negligible contributions from  $s$  and  $p$  wave contributions. The polarized case only contains odd partial waves.

where  $S_{ii}(Elm)$  is the diagonal S matrix element required for Eq. (8). In order to determine the relationship between  $\zeta_{lm}e^{2i\delta_{lm}}$  and  $S_{ii}(E, lm)$  we solve the Schrödinger equation analytically in the limit  $R_{\text{sr}} \rightarrow 0$  using the solutions from [45]. Alternatively, the Schrödinger equation can be solved numerically.

The left panel of Fig. 5 shows the total loss rate coefficient summed over  $l$  and  $m$  for collisions between fermionic  $^{40}\text{K}^{87}\text{Rb}$  molecules in the  $v = 0$ ,  $J = 0$  rovibrational state of the  $X^1\Sigma^+$  potential as a function of the short-range parameters  $\zeta$  and  $\delta$  at a collision energy of  $E/k_B = 350$  nK. For this figure we assume that  $\zeta_{lm} \equiv \zeta$  and  $\delta_{lm} \equiv \delta$  are independent of  $l$  and  $m$ . This rate coefficient can be compared with experimental data on an “unpolarized” sample of this fermionic KRb molecule with at least two equally-populated nuclear-hyperfine states. The right panel shows the loss rate coefficient at  $E/k_B = 350$  nK for a “polarized” sample where all molecules are in the same nuclear hyperfine state and only odd partial wave scattering is allowed. In fact, for this collision energy only the  $p$  wave is significant. The  $p$  wave loss rate is much smaller than that for the  $s$  wave, since the centrifugal barrier is larger than the 350 nK collision energy and the  $p$ -wave loss rate is reduced. We use  $C_6^{\text{iso}} = 16133$  a.u. for both panels.

The most striking observation of Fig. 5 is the appearance of resonances in the loss rate. The origin of this behavior is in the interference between the in- and out-going flux for  $R > R_{\text{sr}}$ . The maximum at  $(\zeta \approx 0.8, \delta \approx 0.6\pi)$  is due to  $s$ -wave collisions and that at  $(\zeta \approx 0.95, \delta \approx 0.9\pi)$  due to  $p$ -wave collisions. In fact, the loss rate is significantly larger than the rate at  $\zeta = 0$  when no flux returns from  $R < R_{\text{sr}}$ . (For  $\zeta = 0$  the loss rate is independent of  $\delta$ .) The loss rate can also be much smaller than at  $\zeta = 0$ . In the limit  $\zeta \rightarrow 1$  we have  $K^{\text{loss}} \rightarrow 0$ . For clarity, this limiting behavior is not shown in the surface plot. If we learn how to change the short range parameter we can envision that a significantly reduction of the loss rate is possible.

Figure 6 shows a comparison of thermally-averaged rate coefficients for ground state  $^{40}\text{K}^{87}\text{Rb}$  molecules with the experimental observations of Ref. [23]. The thermal average assumes a Maxwell-Boltzmann distribution. In order to obtain the comparison we not only assumed that the  $\zeta_{lm}$  and  $\delta_{lm}$  are independent of partial wave but also independent of collision energy over several  $kT$ , where  $k$  is the Boltzmann constant.

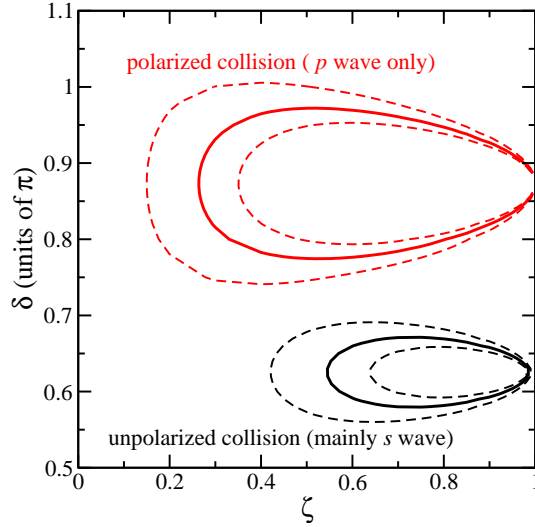


FIG. 6: Bounds on the allowed values of the short-range parameters  $\zeta$  and  $\delta$  from the experimental loss rates obtained in Ref. [23] for either a nuclear spin unpolarized (black curves) or polarized (red curves) sample of  $v = 0$ ,  $J = 0$   $^{40}\text{K}^{87}\text{Rb}$  molecules in the  $X^1\Sigma^+$  potential at a temperature of  $T = 250$  nK. The full lines correspond to pairs of  $(\zeta, \delta)$  where the experimental loss rate agrees with our thermally averaged loss rate. The dashed lines follow from the experimental uncertainty limits. In fact, at a temperature of 250 nK the measured unpolarized loss rate is  $\beta = 1.9(4) \cdot 10^{-10}$   $\text{cm}^3/\text{s}$ , while that for the polarized case is  $\beta = 3.3(7) \cdot 10^{-12}$   $\text{cm}^3/\text{s}$ .

The experimental rates are  $\beta_u = 1.9(4) \cdot 10^{-10}$   $\text{cm}^3/\text{s}$  for the unpolarized case and  $\beta_p = 3.3(7) \cdot 10^{-12}$   $\text{cm}^3/\text{s}$  for the polarized case at a temperature of  $T = 250$  nK. In the experiment  $\beta$  was extracted from the time-dependence of the molecule number density of each nuclear spin state. Consequently, our theoretical loss rate has been multiplied by a factor two for a polarized sample to account for the loss of two molecules per inelastic collision, and multiplied by one(1) for the unpolarized sample as one atom of each nuclear hyperfine state is lost. Ref. [23] verified that the rates for the polarized and unpolarized sample satisfy their  $\beta_u \propto \text{const.}$  and  $\beta_p \propto kT$  Wigner threshold limits as a function of temperature upto  $T \approx 1$   $\mu\text{K}$ .

The figure shows regions in the plane  $(\zeta, \delta)$ , where the theoretical rate coefficient agrees with the experimental rate coefficients within the uncertainties. One region is for the  $p$ -wave dominated polarized case and one for the  $s$ -wave dominated unpolarized case. The two regions do not overlap. Hence, our initial assumption that the short-range parameters are independent of partial wave  $l$  is not valid. The validity of the Wigner threshold limit over collision energies upto a few  $\mu\text{K}$  suggests that the short-range parameters are nevertheless independent of energy over this range. In other words the behavior at  $R < R_{\text{sr}}$ , where a multi-channel description is needed to describe the reactive rearrangement of the atoms, must be captured by more than two parameters. The uncertainty in the dispersion coefficient does not modify this conclusion.

Figure 7 shows the loss rate coefficient for the collision between two bosonic  $^{87}\text{RbCs}$  molecules in the vibrationally excited  $v = 1$ ,  $J = 0$  level of the  $X^1\Sigma^+$  potential at a collision energy of  $E/k = 250$   $\mu\text{K}$  and  $C_6^{\text{iso}} = 142540$  a.u. The nuclear hyperfine states are equally populated and partial waves up to  $l = 8$  are included. We again assume that the short-

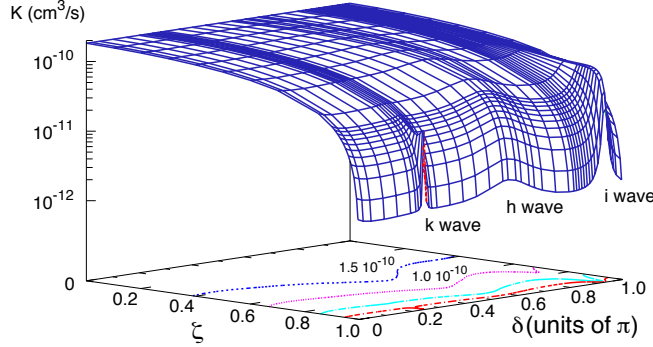


FIG. 7: The total inelastic loss rate coefficient for an unpolarized sample of  $v = 1$ ,  $J = 0$   $^{87}\text{RbCs}$  molecules in the  $X^1\Sigma^+$  potential as a function of the short-range parameters  $\zeta$  and  $\delta$  at a collision energy of  $E/k_B = 250 \mu\text{K}$ . At this collision energy many partial waves contribute.

range parameters are independent of partial wave. In the figure maxima or resonances for  $l = 5, 6$ , and  $7$  are observed. As can be found from a comparison of the binding energies of the  $v = 0$  vibrational levels the three  $\text{RbCs}$ ,  $\text{Rb}_2$ , and  $\text{Cs}_2$  dimer molecules, chemical reaction at ultracold temperature  $\text{RbCs} + \text{RbCs} \rightarrow \text{Cs}_2 + \text{Rb}_2$  is endothermic by  $\approx 40 \text{ cm}^{-1}$  and not energetically allowed. For collisions between  $v = 1$   $\text{RbCs}$  molecules the reaction is exothermic. At a  $250 \mu\text{K}$  collision energy rate coefficients are as large as  $2 \cdot 10^{-10} \text{ cm}^3/\text{s}$  can be seen in Fig. 7. With typical densities in ultracold experiments around  $10^{11} \text{ 1/cm}^3$  to  $10^{12} \text{ 1/cm}^3$  lifetimes as short as a 10 ms could be observed.

## V. CONCLUSION

We have performed a theoretical study critical for the physical realization of highly controlled ultracold molecular systems. In particular, we focused on hetero-nuclear  $\text{KRb}$  and  $\text{RbCs}$  molecules used in ongoing ultracold experiments. Our detailed calculations of  $C_6$  dispersion coefficients for interactions between molecules or molecules with atoms helped the experimental [23] and theoretical [24] efforts to quantitatively describe quantum-state controlled chemical reactions.

Analyses of the isotropic and anisotropic interaction potentials of ultracold polar molecules unveiled a significant contribution from dipole coupling to electronically excited states. This leads to a dramatic change in the interaction potentials as compared to previous estimates based solely on the permanent dipole moment.

Our scattering calculations predict constructive and destructive interferences in the molecular scattering loss rates as a function of short-range parameters. Comparison to recent experimental measurements [23] shows that the initial assumption that the short-range parameters are independent of partial wave  $l$  is not valid.

## VI. ACKNOWLEDGEMENTS

This work is supported by Air Force Office of Scientific Research MURI on Ultracold Molecules. The author acknowledges helpful discussions with Piotr Zuchowski and Eite

Tiesinga.

- 
- [1] J. Sage, S. Sainis, T. Bergeman, and D. DeMille, Phys. Rev. Lett. **94**, 203001 (2005).
  - [2] K.-K. Ni, S. Ospelkaus, M. H. G. de Miranda, A. Peer, B. Neyenhuis, J. J. Zirbel, S. Kotochigova, P. S. Julienne, D. S. Jin, and J. Ye, Science **322**, 231 (2008).
  - [3] M. Baranov, L. Dobrek, K. Goral, L. Santos, and M. Lewenstein, Physica Scripta, **T102**, 74 (2002).
  - [4] K. Goral, L. Santos, and M. Lewenstein, Phys. Rev. Lett. **88**, 170406 (2002).
  - [5] C. Ticknor and J. L. Bohn, Phys. Rev. A **72**, 032717 (2005).
  - [6] R. V. Krems, Int. Rev. Phys. Chem. **24**, 99 (2005).
  - [7] A.V. Avdeenko, M. Kajita, and J. L. Bohn, Phys. Rev. A **73**, 022707 (2006).
  - [8] S. Rohen, D. C. E. Bortolotti, D. Blume, and J. L. Bohn, Phys. Rev. A **74**, 033611 (2006).
  - [9] A. Micheli, G. K. Brennen, and P. Zoller, Nature Physics **2**, 341 (2006)
  - [10] M. Lewenstein, Nature Physics **2**, 309 (2006).
  - [11] A.V. Avdeenko and J. L. Bohn, Phys. Rev. Lett. **90**, 043006 (2003).
  - [12] A.V. Avdeenko, D. C. E. Bortolotti, and J. L. Bohn, Phys. Rev. A **69**, 012710 (2004).
  - [13] T. Rom, T. Best, O. Mandel, A. Widera, M. Greiner, T. W. Hänsch, and I. Bloch, Phys. Rev. Lett. **93**, 073002 (2004).
  - [14] G. Thalhammer, K. Winkler, F. Lang, S. Schmid, R. Grim, and J. Hecker-Denschlag, Phys. Rev. Lett. **96**, 050402 (2006).
  - [15] H. P. Büchler, A. Micheli, and P. Zoller, Nature Physics **3**, 726 (2007).
  - [16] H. P. Büchler, E. Demler, M. Lukin, A. Micheli, N. Prokof'ev, G. Pupillo, and P. Zoller, Phys. Rev. Lett. **98**, 060404 (2007).
  - [17] A. V. Gorshkov, P. Rabl, G. Pupillo, A. Micheli, P. Zoller, M. D. Lukin, and H. P. Büchler, Phys. Rev. Lett. **101**, 073201 (2008).
  - [18] G. Pupillo, A. Micheli, H.P. Büchler, and P. Zoller, *Cold molecules: Creation and applications*, Edited by R. V. Krems, B. Friedrich and W. C. Stwalley, published by Taylor & Francis.
  - [19] E. R. Hudson, N. B. Gilfoy, S. Kotochigova, J. M. Sage, and D. DeMille, Phys. Rev. Letter **100**, 203201 (2008).
  - [20] J. P. Gaebler, J. T. Stewart, J. L. Bohn, and D. S. Jin, Phys. Rev. Letter **98**, 200403 (2007).
  - [21] J. J. Zirbel, K.-K. Ni, S. Ospelkaus, J. P. D'Incao, C. E. Wieman, J. Ye, and D. S. Jin, Phys. Rev. Lett. **100**, 143201 (2008).
  - [22] S. Ospelkaus, K.-K. Ni, M. H. G. de Miranda, B. Neyenhuis, D. Wang, S. Kotochigova, P. S. Julienne, D. S. Jin, and J. Ye, Faraday Discussions, **142**, 351-359, Royal Society of Chemistry, UK (2009).
  - [23] S. Ospelkaus, K.-K. Ni, D. Wang, M. H. G. de Miranda, B. Neyenhuis, G. Guéméner, P. S. Julienne, J. L. Bohn, D. S. Jin, J. Ye, Science **327**, 853 (2010).
  - [24] Z. Idziaszek and P. S. Julienne, arXiv:0912.0370v1 (2009).
  - [25] P. F. Weck and N. Balakrishnan, Int. Rev. Phys. Chem. **25**, 282 (2006).
  - [26] J. M. Hutson and P. Soldan, Int. Rev. Phys. Chem. **26**, 1 (2007).
  - [27] R. V. Krems, W. C. Stwalley, and B. Friedrich, *Cold molecules: theory, experiment, applications*, CRC Press, Taylor and Francis Group, (London, 2009).
  - [28] R. V. Krems, Phys. Chem. Chem. Phys. **10**, 4079 (2008).
  - [29] J. Aldegunde, M. P. de Miranda, J. M. Haigh, B. K. Kendrick, V. Sáez- Rábans, and F. J.

- Aoiz, J. Phys. Chem. A **109**, 6200 (2005); J. Aldegunde, J. M. Alvariño, M. P. de Miranda, V. Sáez Rabanos, and F. J. Aoiz, J. Chem Phys. **125**, 133104 (2006).
- [30] J. M. Alvariño, V. Aquilanti, S. Cavalli, S. Crocchianti, A. Laganà, and T. Martínez, J. Chem. Phys. **107**, 3339 (1997); J. Aldegunde, J. M. Alvariño, D. De Fazio, S. Cavalli, G. Grossi, and V. Aquilanti, Chem. Phys. **301**, 251 (2004).
- [31] T. V. Tscherbul and R. V. Krems, J. Chem. Phys. **129**, 034112 (2008).
- [32] N. Balakrishan and A. Dalgarno, Chem. Phys. Lett. **341**, 652 (2001).
- [33] E. Bodo, F. A. Gianturco, N. Balakrishan, and A. Dalgarno, J. Phys. B **37**, 3641 (2004).
- [34] P. S. Julienne and F. H. Mies, J. Opt. Soc. Am. B **6**, 2257 (1989).
- [35] C. Orzel, M. Walhout, U. Sterr, P. S. Julienne, and S. L. Rolston, Phys. Rev. A **59**, 1926 (1999).
- [36] R. Barnett, D. Petrov, M. Lukin, and E. Demler, Phys. Rev. Lett. **96**, 190401 (2006).
- [37] A. J. Stone, *The theory of intermolecular forces*, (Clarendon Press, London, 1996).
- [38] D. M. Brink and G. R. Satchler, *Angular momentum*, (Clarendon Press, London, 1993).
- [39] S. Kotochigova and E. Tiesinga, J. Chem. Phys. **123**, 174304 (2005).
- [40] S. Kotochigova, J. Chem. Phys. **128**, 024303 (2008).
- [41] K. Pilch, A. D. Lange, A. Prantner, G. Kerner, F. Ferlain, H. -C. Nägerl, R. Grimm, and C. Chin, Phys. Rev. A **79**, 042718 (2009).
- [42] S. Kotochigova, P. S. Julienne, and E. Tiesinga, Phys. Rev. A **68**, 022501 (2003).
- [43] A. Derevianko, J. F. Babb, and A. Dalgarno, Phys. Rev. A **63**, 052704 (2001).
- [44] Bo Gao, Phys. Rev. A **62**, 050702(R) (2000).
- [45] Bo Gao, Phys. Rev. A **80**, 012702 (2009).